Global Journal of Sciences

Global Journal of Sciences
Volume 2, Issue 2, 2025, Pages 23-36
DOI: https://doi.org/10.48165/gjs.2025.2203; ISSN: 3049-0456
https://acspublisher.com/journals/index.php/gjs

Research Article

Synthesis, Photophysical Properties and Metal Sensing Potential of Carbon Dots from Fried Onions

Amir Saddiq[1], Izhar Ul Haq Ali Shah[1], Shah Zeb Ullah[2,3,*], Qismat Ullah[1], Safdar Alam[4]

[1]*Department of Chemistry, Kohat University of Science and Technology Kohat, KP Pakistan*
[2]*Department of physics, Kohat University of Science and Technology Kohat, KP Pakistan*
[3]*Department of Physics, Government Postgraduate College Kohat, KP Pakistan*
[4]*Department of Chemistry, Islamia Collage University of Peshawar, KP Pakistan*

ARTICLE INFO

Article History
Received 15 July 2025
Revised 10 Aug 2025
Accepted 29 Aug 2025
Published 29 Sep 2025

Keywords
Quantum dot;
Zinc Sulphate;
Photoluminescence;
Limit of detection;
Biocompatibility.

ABSTRACT

Using onion as a precursor and a simple hydrothermal procedure, we present a novel, straight forward and environmentally friendly method for synthesizing highly luminous carbon dots (CDs). The optical and physiochemical properties of the synthesized CDs were investigated using scanning electron microscopy (SEM), X-ray diffraction (XRD), Fourier transform infrared (FTIR), UV-visible, fluorescence spectroscopy, and elemental analysis. These CDs exhibited excellent aqueous dispersibility, excitation dependent fluorescence emission, and remarkable stability under various conditions such as pH, high ionic strength, and continuous irradiation. Notably, the presence of Fe^{2+} and Cr^{6+} ions result in significant fluorescence quenching. Therefore, the CDs were employed as a fluorescent probe for the selective detection of Fe^{2+} and Cr^{6+} ions, achieving a good linear correlation (R2 = 0.996) in the concentration range of 0-20 µM with a detection limit of 0.31 µM. The detection capability of these CDs for Fe^{2+} and Cr^{6+} was enhanced by their high selectivity, photo stability, and excellent biocompatibility.

1. INTRODUCTION

The term "nanostructure" refers to the study, development, and use of materials with sizes ranging from 1 to 100 nm. The use of nanostructures in the creation of biosensors is becoming increasingly important [1]. Carbon dots CDs were found a relatively new member of the functional nano-material nuclear family that includes nanotubes, graphene and fullerene. Carbon nano-tubes are formed of coaxial graphite layers that's diameter is smaller than 100 nm and wrapped into cylinders. These nanotubes have very good electrical properties and can also transmit heat. Because of their metallic properties, carbon nanotubes are commonly used as biosensors. Water soluble structures may be created by fictionalizing the surface of carbon nanotubes [2]. Quantum dots have a high resistance to degrading chemical substances and are resistant to light bleaching [2]. Recent trends in various CD applications such as sensing, imaging, nano-medicine, photo-catalysis, photo-voltaic, and optoelectronics are explored, as well as future prospects. Zero-

*Corresponding author. Email: shahzebkhan2917@gmail.com

dimensional CDs are a relatively new introduction to the useful nano-material nuclear family that includes nanotubes, fullerene, graphene and nano diamonds, [3, 4]. These almost spherical particles, which have dimensions ranging from 2 to 20 nm, were brought to the surface in 2004 during the purgation of single-walled carbon nano-tubes produced by the arc-discharge technique [5, 6]. In a typical CD, three separate areas may be distinguished based on photoluminescence emission [7]. Several processes, incorporating quantum confinement, surface states, flaws and molecule states, and cross-linked increased molecular effect, have been postulated throughout the years to describe the PL of the CDs, and a consensus technique has yet to be determined [8, 9]. The quantum confinement effect is observed. The electrons adjust their energy in order to adapt to the decreasing particle size. Some research has reported results matching to the range of fluorescence emission that corresponds to particle size [9]. In addition to the preceding, various investigations in the literature show that CD PL emissions are directly connected to the combination of the aforementioned aromatic sp^2 effect as well as the surface state of the CDs [10]. Zhu along with his colleagues observed that the presence of -COOH and -NH2 groups impacted the pH-dependent behavior of hair fiber-based CDs [11]. For the manufacturing of CDs, used organic fluorophores as initial or starting agent, molecular state emission occurs [12]. Among the synthesis processes for CDs are earc discharge and electrochemical oxidation [13], Hydrothermal synthesis, laser ablation [14], pyrolysis [12], microwave-assisted heating [15]. Other ground-breaking research has focused on the simple and fast microwave treatment strategy for producing CDs from various precursors such as hydrocarbons, carboxylic acids, esters, and biomass wastes [16, 17].

This study involves the synthesis of carbon dots (CDs) derived from light and deep-fried onion, with characterization by UV-Vis, fluorescence, FTIR spectroscopy, and SEM. The synthesized CDs are then employed as a fluorescent probe for the dual detection of Cr^{6+} and Fe^{2+} ions, utilizing the selective quenching and enhancement of their fluorescence.

2. MATERIALS AND METHOD

2.1. Reagents as well as materials

All the reagents of hydrogen peroxide, ammonia, methanol, copper, chromium and lead were derived from Sigma-Aldrich. For the same purpose, double distilled water was utilized for making different solutions used.

2.2. Instrumentation

The following is a summary of the apparatuses used:

For mass estimate, the digital balance (A, R, 139 U.S.A.) is used. Weighing tiny quantities of artificial compounds (up to 0.00001g) is done using an analytical balance (OHOUS, AR, 2130, U.S.A.). Between 200 and 800 nm, ultraviolet-visible spectroscopy (Shimdzu, UV, 1,800, Japan) is used. For drying and warming, a Schwa Bach FRG Memmert D-91216 electric oven is utilized. Fourier transform infrared spectroscopy (in the range of 4500-500/cm) estimate using an FTIR spectrophotometer (model: 300 MX/USA) PL The electrical structure and optical characteristics of materials can be discovered via spectroscopy. Scanning electron microscope (SEM) Confirmation of the morphology, shape, and size of carbon dots X-ray diffraction Spectra It serves as verification for the typical size of crystal carbon dots.

2.3. Samples Collection The samples were collected from the local market of district Karak KPK Pakistan.

2.4. Sample Preparation

Onions were obtained from a local market and washed with distilled water and fried in oil. Before storing fried onions at 4 °C, these were pulverized in a Ball Mill (RETSCH PM 100) as well as shifted through a 60 to 80 wire mesh.

2.5. Synthesis of CDs

Fried onions were washed thoroughly with *n*-hexane for the removal of oil. Then 10 mL of distilled water was added to 1g of finely crushed fried onion, shake and stirred for 30 minutes, cooled down and filtered through sintered glass filter, got a brown liquid and centrifuged it for about 12 minutes at 4000 r.p.m. to eliminate any insoluble particles before being filtered. The stock solution was kept at 4°C in the dark after filtering [18].

2.6. Selectivity and Sensitivity in the Detection of Cr^{6+}

Several tests were carried out to examine the influence of Cr^{6+} on the fluorescence intensity of CDs. Firstly, the CDs' selectivity in a way to six common metal ions, namely Al^{3+}, Fe^{2+}, Pb^{2+}, Ni^{2+}, Zn^{2+}, and Cu^{2+}, was investigated with CDs solution at 200 μM concentrations. The initial fluorescence intensity of CDs is put out by $Cr^{6+}$for about 80% and shows remarkable selectivity towards Cr^{6+} when compared to other metals.

2.7. Method for Detecting Cr^{6+}

A 10 mL calibrated flask was filled with 1.0 mL Tris-HCl buffer solution (10 mM, pH 6.0), a variable amount of Cr^{6+}, and 100 M CDs solution (3 mg mL^{-1}) and diluted to volume with double distilled water. The fluorescence (FL) intensity of the combination solution reached steady state (λ_{ex} = 405 nm, λ_{em} = 506) nm after less than two minutes of incubation. During the quenching procedure, the associated fluorescence emission was recorded.

2.8. UV-VIS spectroscopy

We took 0.1 mL solution of CDs and mixed with 4 mL double distilled water the solution was shaken for 10 minutes. The UV-VIS spectral analysis was then recorded on a Jasco-V670, which 20 was produced in the United States by JASCO. CDs were scanned at wavelengths ranging from 200 to 800 nm [19].

2.9. Photoluminescence spectroscopy

The spectra were collected using a Jasco FP-8500 Spector-fluorimeter (JASCO, USA) from 350-580 nm. The wavelengths of excitation were 325 nm [20].

3. RESULTS AND DISCUSSION

3. 1. UV/Vis Spectral analysis of CDs Synthesized from Fried Onions

CDs had a strong broad bend at 280 nm in the Spectrum of UV-vis absorption as shown in figure 1a and 1b, which was attributable to π-π* aromatic sp^2 hybridization and the conjugation C=C bonds (CC=C-C=C) of this peak [21]. The CDs emit a blue-green colour and show maximum emission at 414 nm to 432 nm, when exposed to a ratio of 365 nm UV lamp, reference from Figure 1 inset.

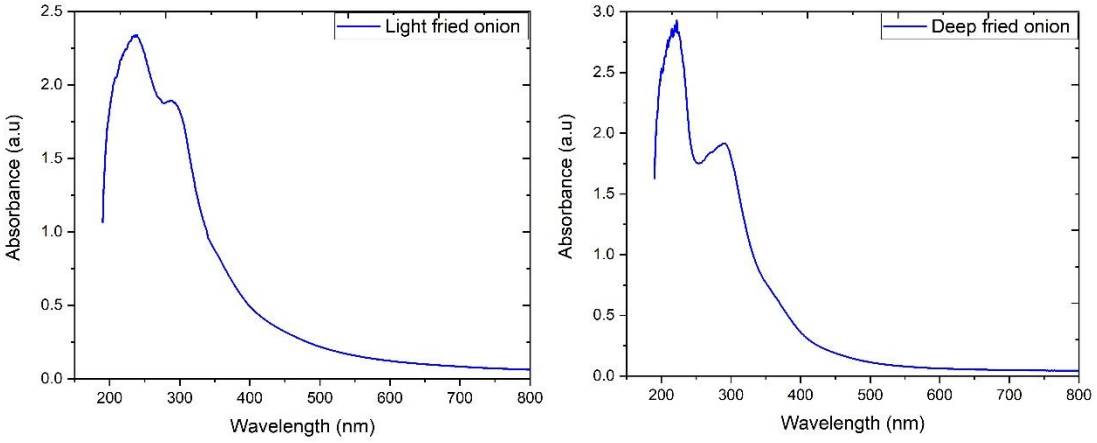

Fig. 1 UV-Vis spectra of CDs of (a) light fried onion and (b) deep fried onion

Overall, the results showed that onion-derived CDs have favorable fluorescence characteristics. In a way, if we deploy the CDs in the field, PL intensity stability will be an important aspect in their deployment. The intensity of PL was tested in contrast to the altering pH and ionic strength to further examine this. The highest intensity of PL was found at pH6, with the bottom rate being found at pH3 as well as 11 (shown Fig. 1a and 1b). In a way, the change in intensity's relative standard deviation (RSD) was just 3.4 percent, demonstrating that we can use CDs throughout a wide pH range without a major variation in the level of intensity. The fluctuation in fluorescence's intensity with ionic strength was examined after openness for different concentrations in NaCl solutions (Figure 4.4 b). The intensity of PL was comparable to that of the DI water solution (blank) at a maximum salt level of around 200 mM even. The fluorescence of CDs is influenced by their surface functional groups (surface state), size (quantum confinement effect), and the comportment of photo-luminance molecules (molecular state) are pasted to their surface. In a way, if these key pathways are not interfered by ions, the fluorescence intensity will remain constant in the presence of fluctuating ionic strengths. CDs had great colloidal stability against particle-particle attraction forces, as evidenced by their stability at increased salt concentrations [22].

3. 2. FTIR analysis of CDs Synthesized from Fried Onions

Figure 2 displays the FTIR analysis of the onion's surface functioning and the related CDs. The onion-like functional groups on the CDs similar to the amino N-H stretching and phenolic OH vibrations, and the broad engrossment bend at 3310 cm^{-1} related to phenolic-OH and amino N-H stretching vibrations. The C-H exaggerating vibrations are responsible for the feeble absorption bend at 2900 cm^{-1}, while the -C N bond in aromatic cyano compounds is responsible for the peak at 2156 cm^{-1}[23, 24]. In the onion, the -C=O stretching of the aldehyde group is depicted by the absorption grid at 1730 cm^{-1}. This highest level

is seen to be at 1700 cm^{-1} in CDs. The stretching of conjugated aldehyde groups caused a shift in the -C=O peak [25]. The aldehydes form these conjugations during HTC as a result of biomass fractionation and structural aromatization stages. Furthermore, the broad highest point at 1604 cm^{-1} is the aromatic C = C bending vibrational peak [26]. The exaggerated vibration of C-N caused the highest point at 1350 cm^{-1}. The existence of COOH groups on the CDs surface was proven by exaggerating vibration peaks of C–O at 1050 cm^{-1}[27].

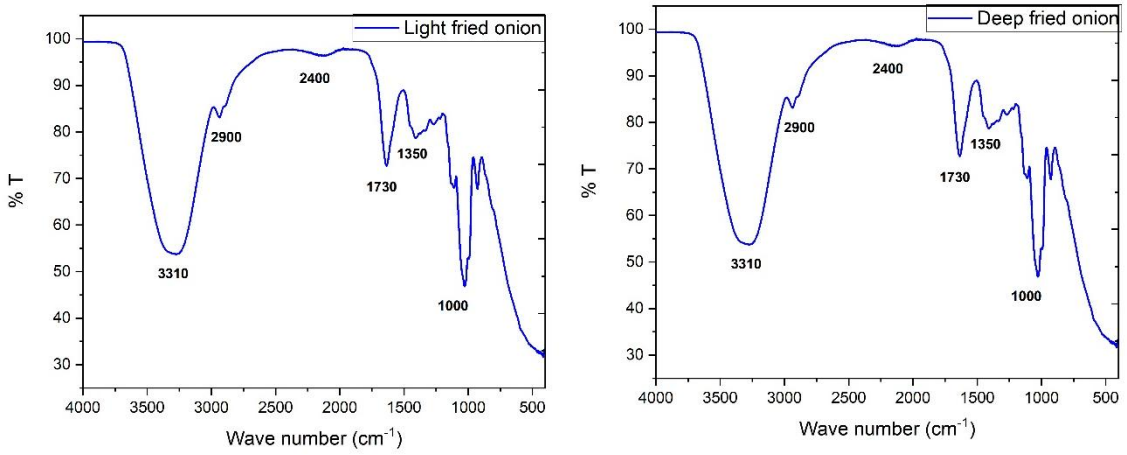

Fig. 2 FTIR analyses of synthesized CDs from (a) deep fried onion and (b) light fried onion

3. 3. XRD Spectroscopy of CDs Synthesized from Fried Onions

The XRD spectroscopy study was carried out in confocal mode with a 532 nm excitation light and under 50 time's magnifications (Figure 3a, 3b). It exhibited two oscillating highest point, one at 1365 cm-1 and the other at 1590 cm-1, which are similar to the cluttered graphitic (G) belt and the (D) graphitic belt of sp2 carbon atoms, consecutively [28]. On the basis of the peak intensity count, the highest ardency proportion (ID/IG) connected to D as well as G peaks were counted up to 0.76. Surface flaws were primarily produced through the companionship of oxygenated groups (C-O, C=O, O-C=O) and were related with sp^2 sites [29]. The limit of crystalline of the produced CDs was founded by XRD patterns. The carbon lattice spacing was indexed to greater broad diffraction peak around 22°, and the peak at 16° shown the existence of chaotic carbon, as seen in (Figure 3a, 3b) [30].

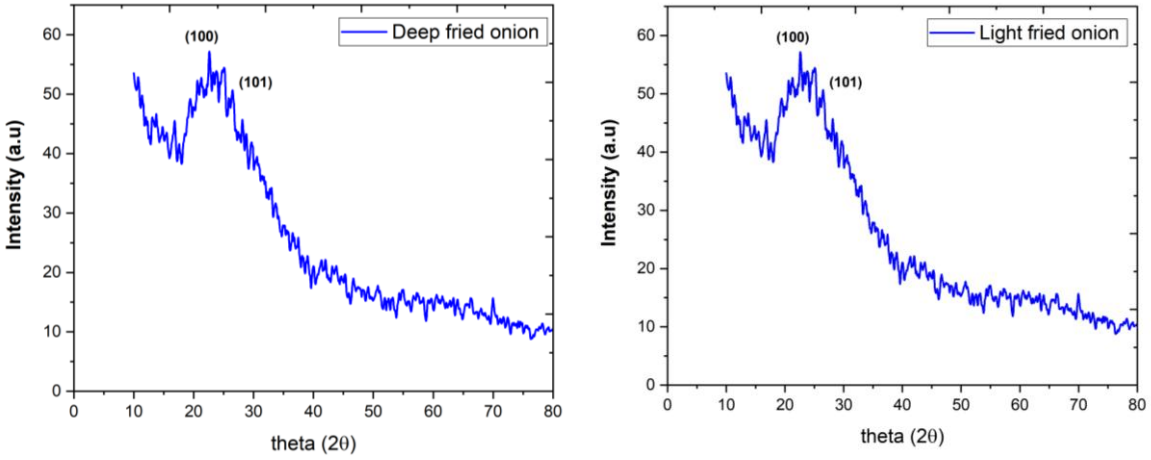

Fig. 3 XRD patterns of synthesized CDs from (a) deep fried onion and (b) light fried onion.

3. 4. SEM analysis of CDs Synthesized from Fried Onions

SEM was utilized to study the morphology of the CDs particles, and the results presented in (Figure 4a) indicated that the CDs were quasi-spherical as well as well scattered. The image of SEM (see Figure 4.4a) revealed a lattice-like spacing of 0.39 nm, confirming the CDs crystalline characteristics and agreeing with the XRD data [31]. Particle diameters varied from 1 to 6 nm, having an average of 3.2 nm (Figure 4b). Furthermore, the carbon, oxygen, and nitrogen elemental mapping distribution on the CD surface (Figure 4c) demonstrated that the elements were equally dispersed.

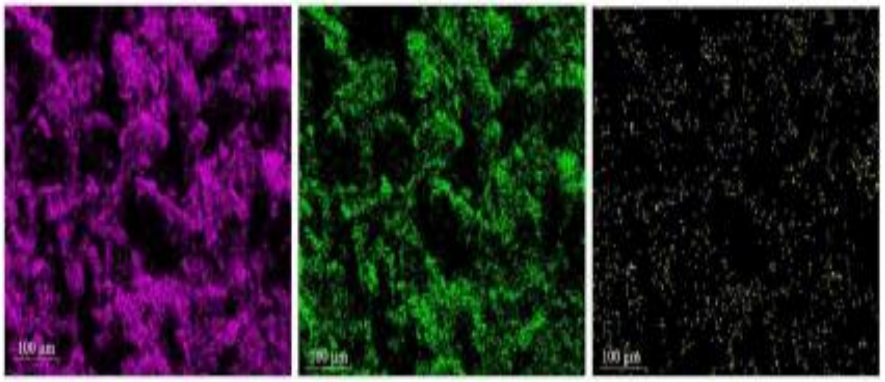

Fig. 4 (a) SEM pictures of CDs, **(b)** SEM-determined particle size distribution of CDs.

3. 5. The effect of various metal ion solutions on CDs

Cu^{2+}, Pb^{2+}, Cr^{6+}, Co^{2+}, Ni^{2+}, Mn^{2+}, as well as Fe^{2+} were chosen as typical cations for assessing cation impacts on CD fluorescence. As seen in Figures 5 and 6. CDs fluorescence emission from deep fried onion and fried appetizers was dramatically decreased by Fe^{2+} and Cr^{6+}, while the other cations had no impact. As a result, CDs respond preferentially to Fe^{2+} and Cr^{6+} in a cation-rich environment. Under tough circumstances, the CDs appear to have a high selectivity for Fe^{2+} and Cr^{6+}. When the FTIR data from the -OH, -COOH, and $–NH_2$ groups on the surface of the manufactured CDs are combined, We may infer that CDs can form stable complexes with Fe^{2+} and Cr^{6+} via -OH, $-NH_2$, and -COOH groups, resulting in fluorescence quenching owing to photo-induced electron transfer and strong selectivity of CDs for Fe^{2+} and Cr^{6+}. (From the left to the right: CDs, CDs+Pb^{2+}, CDs+Cu^{2+}, CDs+Co^{2+}, CDs+Ni^{2+}, CDs+Mn^{2+}, CDs+Cr^{6+}, CDs+Fe^{2+})

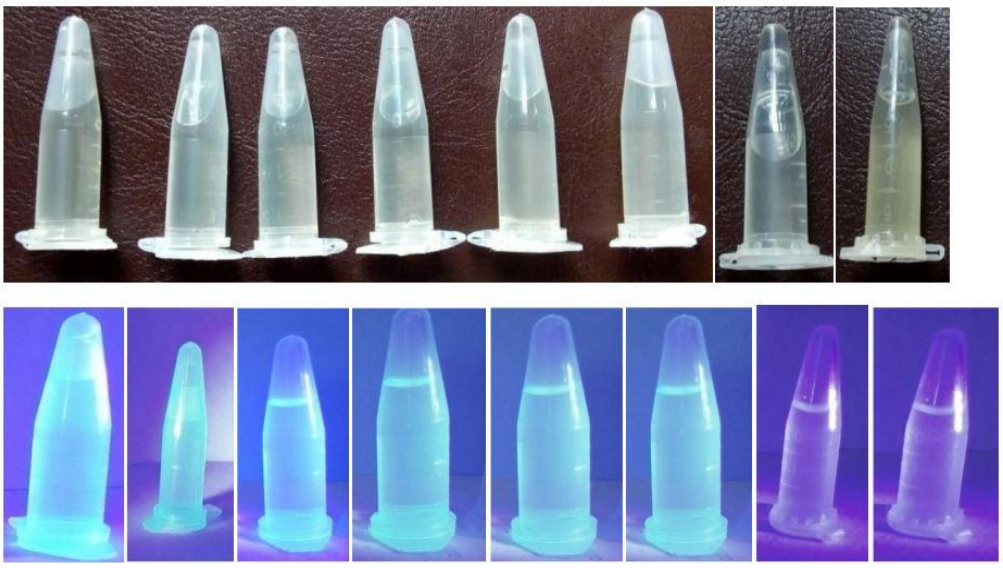

Fig. 5 CDs of light fried onions containing metal ions under day and UV light (From the left to the right: CDs, CDs+Pb^{2+}, CDs+Cu^{2+}, CDs+Co^{2+}, CDs+Ni^{2+}, CDs+Mn^{2+}, CDs+Cr^{6+}, CDs+Fe^{2+})

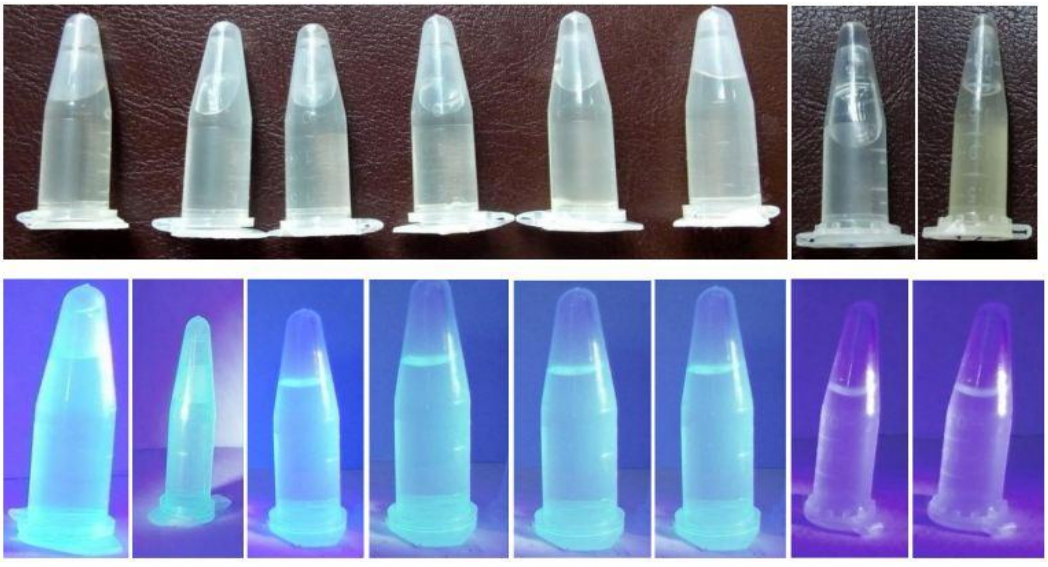

Fig. 6 Deep-fried onion CDs containing metal ions exposed today and UV light

3. 6. CDs PL spectroscopy generated from (a) deep fried onion and (b) light fried onion at different excitation.

Another optical approach for proving the production of CDs is the characteristic emission analysis performed by fluorescence spectroscopy. A large number of emitting fluorescence spectrum based on the excitation wavelength was discovered, as shown in Figure 4.6 a land and different particles sizes of synthesized CDs were attributed also with the functional groups on the surface creating trap states [32]. The highest fluorescence reduction was red, shifted from 350-550 nm after increasing the excitation

wavelength from 340 - 460 nm. Furthermore, a high level fluorescence emission was recorded at a 360 nm excitation wavelength, which corresponded to blue emission, while the last peak was seen at roughly 500 nm (emission), which belonged to green emission [33]. Nitrogen doping was causing the blue emission in the graphitic structure, whereas carboxyl (-COOH) and aldehyde (-HC=O) groups were causing mostly Green Emission, which boosted the green fluorescence emission center's [34, 35].

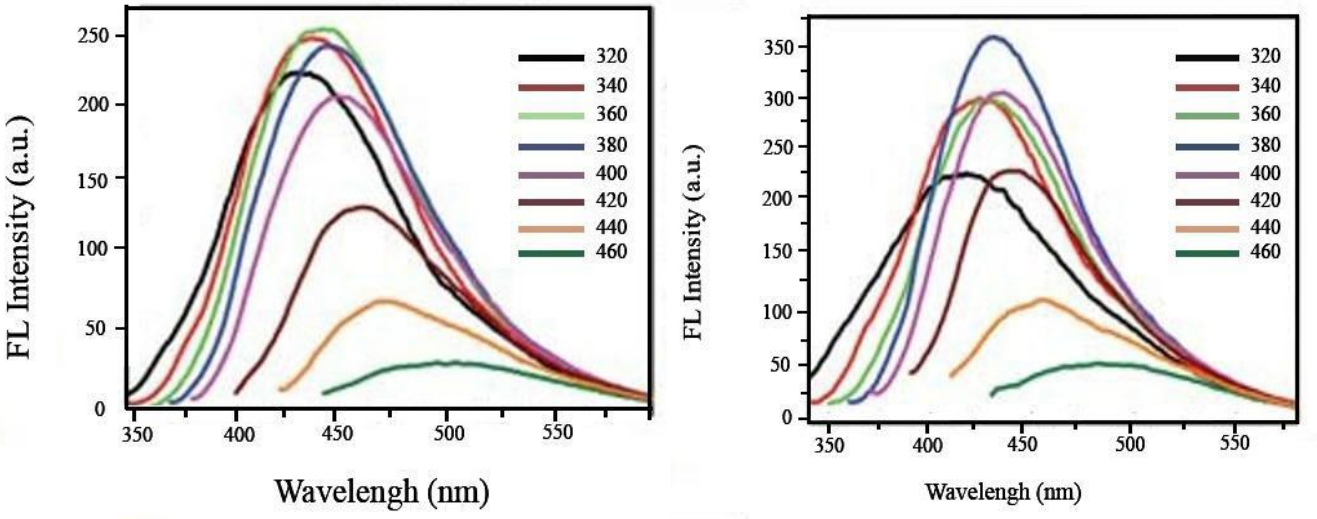

Fig.7 CDs PL intensity produced from (a) light fried onion and (b) deep fried onion at various levels of excitation.

3. 7. A quantitative examination of CDs manufactured from (a) light fried onion and (b) deep fried onion with Fe^{2+} ion using PL.

To investigate the detection sensitivity of CDs in Tris-HCl buffer solutions with a pH of 7 and Fe^{2+} concentrations ranging from 0 to 24 M, CDs were exposed to a range of concentrations ranging from 0 to 24 M of light fried onion and 0 to 42 M was added to deep-fried onion CDs. As demonstrated in Figure 4.6 (a) and (b), as the concentration of Fe^{2+} increased, the intensity of the CDs decreased. The correlation between concentrations of Fe^{2+} on the x-axis and (F0-F)/F0 on the y-axis in light fried onion CDs was found to be in the range of 2–12 M (R2 = 0.9905) in light fried onion CDs and 2-16 M (R2 = 0.9577) in deep fried onion CDs. Figures 4.6 (c) and (d). The limits of detection (LOD) and quantization (LOQ) of light fried onion CDs were determined by computing using the three times the standard deviation rule (LOD = 3/s) to be 2.68 M and 8.94 M, respectively. Deep fried onions CDs were estimated to be 6.61 million and 20.83 million. When the proposed CDs-based approaches for Fe^{2+} detection are compared to previously published methods, it is clear that this CDs-based method is superior or equal to those previously reported in the literature.

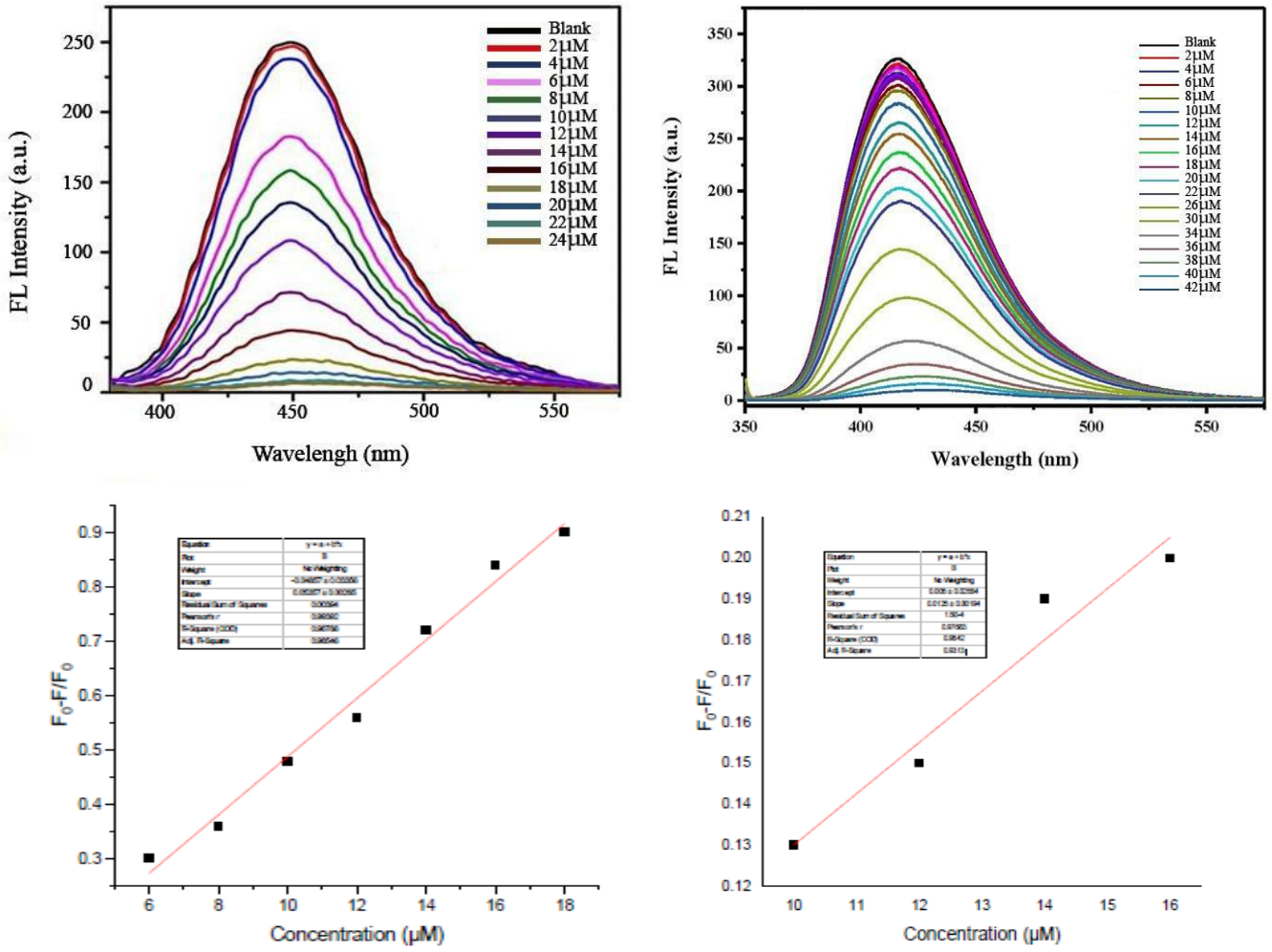

Fig. 8 CDs with high PL intensity (a) deep fried onion as well as (b) light fried onion with various concentration of Fe^{2+} (c) the linear association between (Fo-F)/Fo and Fe^{2+} content in deep fried onion CDs (d) the linear association between (Fo-F)/Fo and the Fe^{2+} content in light fried onion CDs

3. 8. Quantitative investigation of CDs produced from deep fried onion and light fried onion with Cr^{6+} ion using PL.

To evaluate the sensitivity of CD detection in Tris-HCl buffer solutions with a pH of 7 and Cr^{6+} concentrations ranging from 0 to 26 M was added to CDs of deep-fried onion and 0 to 28 M CDs of light fried onion were added. As seen in Figures 4.7 (a) and 4.7 (b), as the concentration of Cr^{6+} increased, the intensity of the CDs emission decreased. A powerful linear connection the relationship between the concentration of Cr^{6+} on the x-axis and the concentration of Cr^{6+} on the y-axis and $(F_0\text{-}F)/F_0$ on the y-axis in Deep fried onion CDs were found to be in the range of 2–12 M (R2 = 0.9905) while light fried onion CDs were found to be in the range of 2-16 M (R2 = 0.9577). (See Figures 4.8 (c) and (d)) (d). the limits of detection (LOD) and quantification (LOQ) of light fried onion CDs were found to be 5.9 M and 16.6 M, respectively. Based on the three times the standard deviation rule (LOD = 3/s), while CDs of light fried onion were calculated to be 2.8 M and 7.08 M, respectively [36].

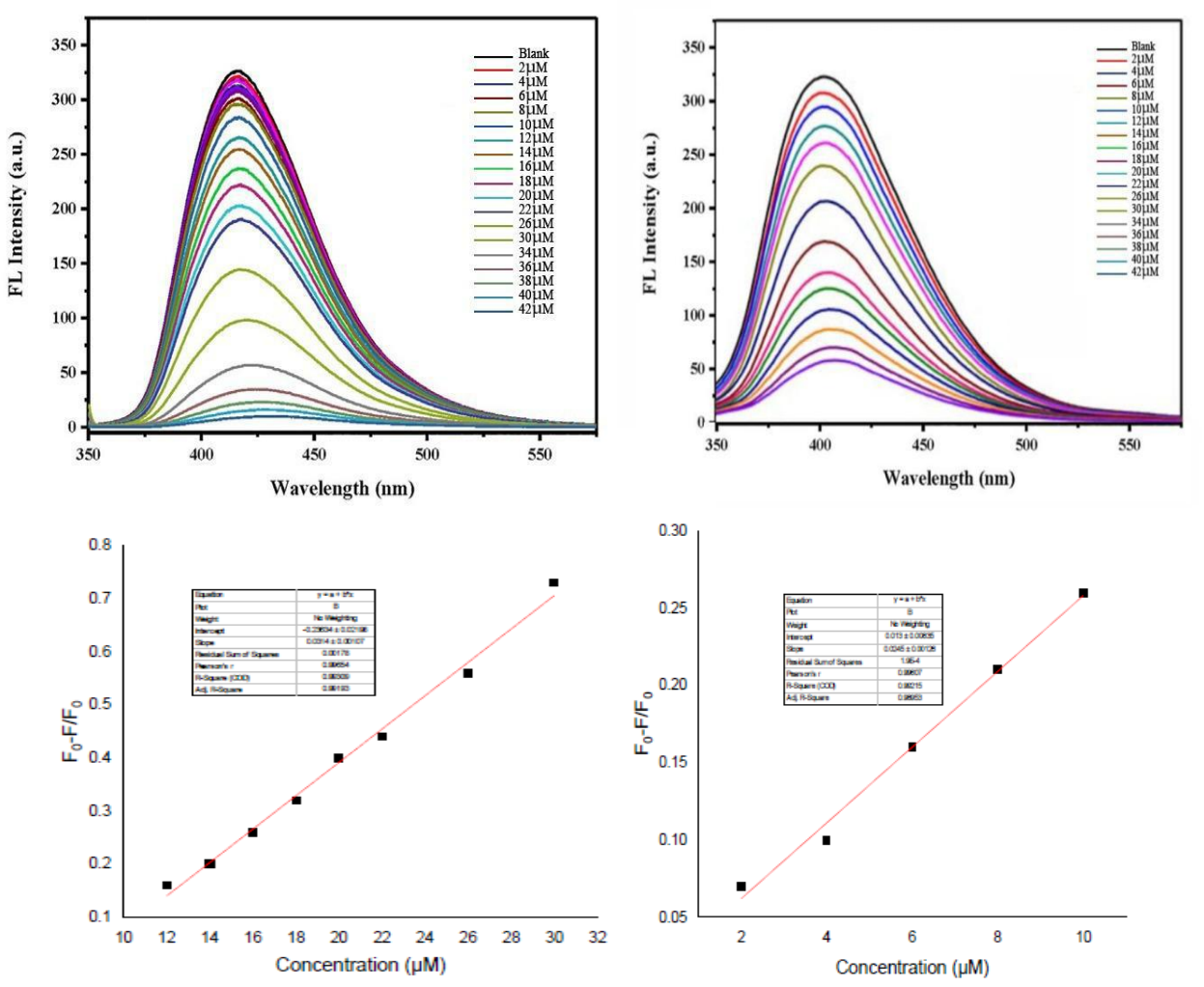

Fig. 9 CDs PL intensity of (a) deep fried onion as well as (b) light fried at various concentration of Cr^{6+} (c) the linear association between $(F_o\text{-}F)/FO$ and Cr^{6+} concentration in deep fried onion CDs (d) the linear association between $(Fo\text{-}F)/F_O$ and Cr^{6+} content in light fried onion CDs

3. 9. The Mechanism

The phenomenon of CDs fluorescence quenching have prompted a great deal of discussion in scientific literature. To begin, the presence of significant number of carboxyl, hydroxyl, and nitrogenous groups on the surface of CDs may boost the chance of non-radioactive exactions recombination. When the Fe^{2+} ions come into touch with these functional groups the quenching effects arise as a consequence of the coordination process between the two things that were CDs functional groups and the metal ions, resulting in an increased chance of non-radioactive recombination of the exactions. Second, the quenching process is responsible for the nonradioactive electron-hole annihilation activity between CDs and Fe^{2+}. The dealing of carbon dots with metal ions, in particular, causes the d orbital of Fe^{2+} to split, leading in the transfer of CDs excited state electrons to Fe^{2+} half-filled 3d orbital's and the quenching of CDs [36].

4. Conclusions

In this examination, CDs were successfully prepared by hydrothermal process from fried onions which are ecofriendly, non-toxic and good tunable. The synthesized CDs had been characterized by UV-Vis, FT-IR, SEM, XRD and PL techniques. The present work concluded that CDs were successfully synthesized were used for detection of Fe^{2+} and Cr^{6+} in aqueous solution. CDs exhibited a substantial broad bend at 280 nm in the UV-vis absorption spectrum. This bend was caused by π-π^* aromatic sp^2 hybridization and the conjugation C=C bonds (C-C=C-C=C) of this peak. The CDs produce a blue-green color and peak at 414–432 nm when exposed to a UV light with a wavelength of 365 nm. FTIR analysis confirmed the presence of onion-derived surface groups on the CDs. Key bands included O-H/N-H stretch at 3310 cm^{-1}, C-H stretch at 2900 cm^{-1}, -C≡N at 2156 cm^{-1}, and a shifted C=O stretch (from 1730 cm^{-1} in onion to 1700 cm^{-1} in CDs), indicating conjugated aldehyde groups. SEM analysis revealed quasi-spherical, well-scattered CDs with an average diameter of 3.2 nm (range 1–6 nm). A lattice spacing of 0.39 nm confirmed their crystalline nature, consistent with XRD data. The fluorescence emission exhibited a red shift from 350 to 550 nm as the excitation wavelength increased from 340 to 460 nm. Maximum emission intensity was observed at 360 nm (blue) and 380 nm for light and deep fried respectively.

Author Contribution

All authors contributed equally to the conception, analysis, and writing of this work. All authors approved the final version of the manuscript.

Conflicts of Interest

The author declares no conflicts of interest.

Funding

This research received no external funding.

Data Availability Statement

All data relevant to the study are included in the article.

REFERENCES

[1] Vo-Dinh, T., Cullum, B. M., & Stokes, D. L. (2001). Nanosensors and biochips: frontiers in biomolecular diagnostics. *Sensors and Actuators B: Chemical*, 74, 2–11.

[2] Medintz, I. L., Uyeda, H. T., Goldman, E. R., & Mattoussi, H. (2005). Quantum dot bioconjugates for imaging, labelling and sensing. *Nature Materials*, 4, 435–446.

[3] Gan, Z., Xu, H., & Hao, Y. (2016). Mechanism for excitation-dependent photoluminescence from graphene quantum dots and other graphene oxide derivates: consensus, debates and challenges. *Nanoscale*, 8, 7794–7807.

[4] Goryacheva, I. Y., Sapelkin, A. V., & Sukhorukov, G. B. (2017). Carbon nanodots: mechanisms of photoluminescence and principles of application. *TrAC Trends in Analytical Chemistry*, 90, 27–37.

[5] Sun, X., & Lei, Y. (2017). Fluorescent carbon dots and their sensing applications. *TrAC Trends in Analytical Chemistry*, 89, 163–180.

[6] Zhang, J., & Yu, S.-H. (2016). Carbon dots: large-scale synthesis, sensing and bioimaging. *Materials Today*, 19, 382–393

[7] Basu, N., & Mandal, D. (2019). Time-resolved photoluminescence of pH-sensitive carbon dots. *Carbon*, 144, 500–508.

[8] Yuan, F., Zheng, X., Johnston, A., Wang, Y.-K., Zhou, C., Dong, Y., et al. (2020). Color-pure red light-emitting diodes based on two-dimensional lead-free perovskites. *Science Advances*, 6, eabb0253.

[9] Li, H., He, X., Kang, Z., Huang, H., Liu, Y., Liu, J., et al. (2010). Water-soluble fluorescent carbon quantum dots and photocatalyst design. *Angewandte Chemie International Edition*, 49, 4430–4434.

[10] Zuo, J., Jiang, T., Zhao, X., Xiong, X., Xiao, S., & Zhu, Z. (2015). Preparation and application of fluorescent carbon dots. *Journal of Nanomaterials*, 2015, 10–10.

[11] Shamsipur, M., Barati, A., Taherpour, A. A., & Jamshidi, M. (2018). Resolving the multiple emission centers in carbon dots: from fluorophore molecular states to aromatic domain states and carbon-core states. *The Journal of Physical Chemistry Letters*, 9, 4189–4198.

[12] Bourlinos, A. B., Stassinopoulos, A., Anglos, D., Zboril, R., Karakassides, M., & Giannelis, E. P. (2008). Surface functionalized carbogenic quantum dots. *Small*, 4, 455–458.

[13] Cailotto, S., Amadio, E., Facchin, M., Selva, M., Pontoglio, E., Rizzolio, F., et al. (2018). Carbon dots from sugars and ascorbic acid: role of the precursors on morphology, properties, toxicity, and drug uptake. *ACS Medicinal Chemistry Letters*, 9, 832–837.

[14] Dimos, K. (2016). Carbon quantum dots: surface passivation and functionalization. *Current Organic Chemistry*, 20, 682–695.

[15] Yang, S., Sun, J., Li, X., Zhou, W., Wang, Z., He, P., et al. (2014). Large-scale fabrication of heavy doped carbon quantum dots with tunable-photoluminescence and sensitive fluorescence detection. *Journal of Materials Chemistry A*, 2, 8660–8667.

[16] Wang, X., Fang, X., Yang, P., Jiang, X., Jiang, F., Zhao, D., et al. (2014). The locust genome provides insight into swarm formation and long-distance flight. *Nature Communications*, 5, 2957.

[17] Barman, M. K., Jana, B., Bhattacharyya, S., & Patra, A. (2014). Photophysical properties of doped carbon dots (N, P, and B) and their influence on electron/hole transfer in carbon dots–nickel (II) phthalocyanine conjugates. *The Journal of Physical Chemistry C*, 118, 20034–20041.

[18] Bandi, R., Gangapuram, B. R., Dadigala, R., Eslavath, R., Singh, S. S., & Guttena, V. (2016). Facile and green synthesis of fluorescent carbon dots from onion waste and their potential applications as sensor and multicolour imaging agents. *RSC Advances*, 6, 28633–28639.

[19] D'souza, S. L., Chettiar, S. S., Koduru, J. R., & Kailasa, S. K. (2018). Synthesis of fluorescent carbon dots using Daucus carota subsp. sativus roots for mitomycin drug delivery. *Optik*, 158, 893–900.

[20] Ding, H., Ji, Y., Wei, J.-S., Gao, Q.-Y., Zhou, Z.-Y., & Xiong, H.-M. (2017). Facile synthesis of red-emitting carbon dots from pulp-free lemon juice for bioimaging. *Journal of Materials Chemistry B*, 5, 5272–5277.

[21] Yang, R., Guo, X., Jia, L., Zhang, Y., Zhao, Z., & Lonshakov, F. (2017). Green preparation of carbon dots with mangosteen pulp for the selective detection of Fe^{3+} ions and cell imaging. *Applied Surface Science*, 423, 426–432.

[22] Alimohammadi, M., Sharifi, H., Tashkhourian, J., Vazan, M., Shamsipur, M., & Hemmateenejad, B. (2023). An optical nose based on array of metal-doped carbon dots for identification of hazardous amines and assessing meat freshness. *Sensors and Actuators B: Chemical*, 393, 134274.

[23] Prasannan, A., & Imae, T. (2013). One-pot synthesis of fluorescent carbon dots from orange waste peels. *Industrial & Engineering Chemistry Research*, 52, 15673–15678.

[24] Woodley, S. B., Mould, R. R., Sahuri-Arisoylu, M., Kalampouka, I., Booker, A., & Bell, J. D. (2021). Mitochondrial Function as a Potential Tool for Assessing Function, Quality and Adulteration in Medicinal Herbal Teas. *Frontiers in Pharmacology*, 12, 814.

[25] Titirici, M.-M., White, R. J., Brun, N., Budarin, V. L., Su, D. S., Del Monte, F., et al. (2015). Sustainable carbon materials. *Chemical Society Reviews*, 44, 250–290

[26] Shi, J., Ni, G., Tu, J., Jin, X., & Peng, J. (2017). Green synthesis of fluorescent carbon dots for sensitive detection of Fe^{2+} and hydrogen peroxide. *Journal of Nanoparticle Research*, 19.

[27] Mehta, V. N., Jha, S., Basu, H., Singhal, R. K., & Kailasa, S. K. (2015). One-step hydrothermal approach to fabricate carbon dots from apple juice for imaging of mycobacterium and fungal cells. *Sensors and Actuators B: Chemical*, 213, 434–443.

[28] Edison, T. N. J. I., Atchudan, R., Shim, J.-J., Kalimuthu, S., Ahn, B.-C., & Lee, Y. R. (2016). Turn-off fluorescence sensor for the detection of ferric ion in water using green synthesized N-doped carbon dots and its bio-imaging. *Journal of Photochemistry and Photobiology B: Biology*, 158, 235–242.

[29] Li, H., Kang, Z., Liu, Y., & Lee, S.-T. (2012). Carbon nanodots: synthesis, properties and applications. *Journal of Materials Chemistry*, 22, 24230–24253

[30] Xu, H., Xie, L., & Hakkarainen, M. (2017). Coffee-ground-derived quantum dots for aqueous processable nanoporous graphene membranes. *ACS Sustainable Chemistry & Engineering*, 5, 5360–5367.

[31] Das, A., Gude, V., Roy, D., Chatterjee, T., De, C. K., & Mandal, P. K. (2017). On the molecular origin of photoluminescence of nonblinking carbon dot. *The Journal of Physical Chemistry C*, 121, 9634–9641.

[32] Baker, S. N., & Baker, G. A. (2010). Luminescent carbon nanodots: emergent nanolights. *Angewandte Chemie International Edition*, 49, 6726–6744.

[33] Sciortino, L., Sciortino, A., Popescu, R., Schneider, R., Gerthsen, D., Agnello, S., et al. (2018). Tailoring the emission color of carbon dots through nitrogen-induced changes of their crystalline structure. *The Journal of Physical Chemistry C*, 122, 19897–19903.

[34] Du, J., Wang, H., Wang, L., Zhu, S., Song, Y., Yang, B., et al. (2016). Insight into the effect of functional groups on visible-fluorescence emissions of graphene quantum dots. *Journal of Materials Chemistry C*, 4, 2235–2242.

[35] Wang, L., Zhu, S.-J., Wang, H.-Y., Qu, S.-N., Zhang, Y.-L., Zhang, J.-H., et al. (2014). Common origin of green luminescence in carbon nanodots and graphene quantum dots. *ACS Nano*, 8, 2541–2547

[36] Lu, M., & Zhou, L. (2019). One-step sonochemical synthesis of versatile nitrogen-doped carbon quantum dots for sensitive detection of Fe^{2+} ions and temperature in vitro. *Materials Science and Engineering: C*, 101, 352–359.